

2-D wave modelling and reverse-time migration by a new finite difference scheme based on the Galerkin method

Xiang Du and John C. Bancroft

SUMMARY

Full wave equation 2-D modeling and migration using a new finite difference scheme based on the Galerkin method are presented. Since it involves semi-discretization by the finite element method (FEM), it is also called finite element and finite difference method (FE-FDM). Using the semi-discretization technique of the finite element method (FEM) in the z direction with the linear element, the original problem can be written as a coupled system of lower dimensions partial differential equations (PDEs) that continuously depend upon time and space in the x direction. A fourth-order finite difference method (FDM) is used to solve these PDEs. The concept and principle are introduced in this paper. Compared with the explicit finite-difference method of the same accuracy, the stability condition is less constrained and shows its advantage over the conventional FDM. An absorbing boundary condition of fourth-order accuracy is used to prevent boundary reflections. In numerical experiments, a comparison is made between a FE-FDM numerical solution and an analytic solution of the quarter-plane. Here, FE-FDM is shown to be accurate in numerical computation; in addition, a constant velocity model with two irregular interfaces is simulated to get the poststack seismic section, which is then successfully migrated. These examples show the potential of FE-FDM in modeling and reverse-time migration.

INTRODUCTION

The finite element–finite difference method (FE–FDM), a numerical method using the FEM and FDM in the spatial domain to solve partial differential equations, was first put forward by Dong (2001). In contrast to FEM, the FE-FDM semi-discretizes the PDE in a partial spatial domain. This yields a coupled system of PDEs, which still depend continuously upon both time and space (although not all the space dimensions), and are solved with FDM. Thus, the strengths of FEM (the adaptation to the arbitrary domain and boundary) are retained. The shortcomings of the FEM (large demand on computer memory and high computation costs) are reduced because of the semi-discretization. In fact, when the lumped global mass matrix of FEM is used and other spatial domains and temporal domain are solved by FDM, it is equivalent to the FDM in nature. So, this method actually is a finite difference scheme based on Galerkin method.

Earlier applications employed semi-discretization along x direction by FEM. However, considering that the spatial sampling interval in the x direction is greater than that in the z direction, the wave equation is semi-discretized along the z direction by the FEM. Another development new to this study is that we employ the fourth order rather second-order FDM for computing along the x direction. This allows us to derive a new and

accurate stability condition for the FE-FDM and we show that it is less constrained compared with a full FDM of the same order. The fourth-order absorbing boundary condition (Clayton and Engquist, 1977) is used to prevent boundary reflections. Some examples of 2-D wave equation modeling and migration are given as well to demonstrate the potential of this method through some comparison with analytical solution and other methods.

PRINCIPLE

Consider the hyperbolic model problem, with the 2-D scalar wave equation:

$$\frac{\partial^2 u}{\partial x^2} + \frac{\partial^2 u}{\partial z^2} = \frac{1}{a^2(x, z)} \frac{\partial^2 u}{\partial t^2}, \quad \text{in } \Omega, \quad (1)$$

where $u(x, z, t)$ denotes the wave displacement in the horizontal coordinate x , vertical coordinate z (where the z axis points downward) and time t , respectively, and $a(x, z)$ is the medium velocity.

FEM semi-discretization in the z direction

Semi-discretizing the vertical coordinate (z) in the region of $[0, Z]$, one constructs a finite element function space as

$$u_h(x, z, t) = \sum_{i=1}^N u_i(t, x) N_i(z), \quad (2a)$$

and a

$$\frac{\partial}{\partial z} u_h(x, z, t) = \sum_{i=1}^N u_i(t, x) \frac{d}{dz} N_i(z) = \sum_{i=1}^N u_i(t, z) B_i(z), \quad (2b)$$

where N is the nodal number. According to the Galerkin method (Lu and Guan, 1987), one can write the semi-discretized PDEs as:

$$M \frac{\partial^2 u}{\partial t^2} + Ku = H \frac{\partial^2 u}{\partial x^2}, \quad (3a)$$

where

$$M = \sum_{n=1}^{N_e} M_e, \quad K = \sum_{n=1}^{N_e} K_e, \quad H = \sum_{n=1}^{N_e} H_e, \quad (3b)$$

$$M_e = \int_e \frac{1}{a(x, z)} N^T N dz, \quad K_e = \int_e B^T B dz, \quad H_e = \int_e N^T N dz. \quad (3c)$$

where e represents the each nod, and N_e is the total number of elements. In this paper, the line element is considered for the semi-discretization along the z direction. The interpolation function is $N(x) = (\xi, 1-\xi)$, here $\xi = \frac{z_{i+1} - z}{l}$, and $l = z_{i+1} - z_i$. It can be seen that the matrices M , K and H are all symmetric and tridiagonal.

$$\begin{aligned}
 u[i]_j^{n-1} - 2u[i]_j^n + u[i]_j^{n+1} &= \frac{(v[i]_j^n \Delta t)^2}{h^2} (u[i]_{j-1}^n - 2u[i]_j^n + u[i]_{j+1}^n) \\
 &+ \frac{(v[i]_{j-1}^n \Delta t)^2}{6l^2} (-u[i-2]_{j-1}^n + 16u[i-1]_{j-1}^n - 30u[i]_{j-1}^n + 16u[i+1]_{j-1}^n - u[i+2]_{j-1}^n) \\
 &+ \frac{4(v[i]_j^n \Delta t)^2}{6l^2} (-u[i-2]_j^n + 16u[i-1]_j^n - 30u[i]_j^n + 16u[i+1]_j^n - u[i+2]_j^n) \\
 &+ \frac{(v[i]_{j+1}^n \Delta t)^2}{6l^2} (-u[i-2]_{j+1}^n + 16u[i-1]_{j+1}^n - 30u[i]_{j+1}^n + 16u[i+1]_{j+1}^n - u[i+2]_{j+1}^n)
 \end{aligned} \tag{5}$$

The local truncation error of this scheme has the form of $O(\tau^2 + l^4)$ (Durrant, 1999). Figure 1 is the temporal and spatial grid computation. In contrast to the central FDM, each grid computation at time $t - \tau$ or $t + \tau$ has a relationship with the fifteen points at t , which will affect the stability condition.

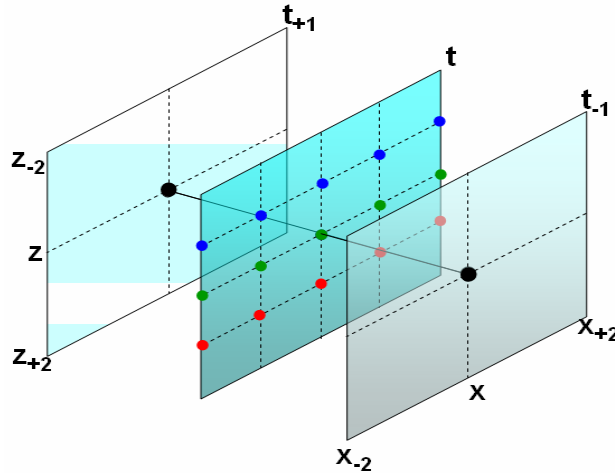


Figure 1. Grid computation in the spatial and time domain

Analysis of stability condition

The computational error can be expanded in a Fourier series as

$$e_{i,j}^n = \sum_p \sum_q \Gamma_{p,q}^n \exp(\imath pi\Delta x) \exp(\imath qj\Delta z), \tag{6}$$

where $\imath = \sqrt{-1}$ and $\Gamma_{p,q}^n$ is a complex coefficient. It is sufficient to consider only a component

$$e_{i,j}^n = \Gamma^n \exp(\imath pi\Delta x) \exp(\imath qj\Delta z). \tag{7}$$

Substituting the Equation (6) into Equation (4), we obtain

$$\Gamma^{n+1} = -\Gamma^{n-1} + 2A\Gamma^n, \tag{8}$$

where

$$A = 1 + g_{i,j}^Z (\cos(q\Delta y) - 1) + \frac{1}{2} g_{i,j}^X \left(-\frac{1}{6} \cos(2p\Delta x)\right) + \frac{16}{6} \cos(p\Delta x) - \frac{30}{6} \left(\frac{4}{6} + \frac{2}{6} \cos(q\Delta y)\right), \quad (9)$$

with $g_{i,j}^Z = \frac{v_{i,j}^2 (\Delta t)^2}{(\Delta z)^2}$, $g_{i,j}^X = \frac{v_{i,j}^2 (\Delta t)^2}{(\Delta x)^2}$. Since A is real, the real part and the imaginary part of Γ^n satisfy the same equation. So we can simply treat Γ^n as a real quantity. Equation 9 is replaced by

$$\gamma^2 - 2Ar + 1 = 0. \quad (10)$$

Stability is assured if $-1 \leq A \leq 1$ as indicated by the computation result of Wu et al. (1996). This requirement on A yields the result that

$$-1 \leq 1 + g_{i,j}^Z (\cos(q\Delta x) - 1) + \frac{1}{2} g_{i,j}^X \left(-\frac{1}{6} \cos(2p\Delta x) + \frac{16}{6} \cos(p\Delta x) - \frac{30}{6} \left(\frac{4}{6} + \frac{2}{6} \cos(q\Delta y)\right)\right) \leq 1 \quad (11)$$

We assume $\bar{g}_{i,j} = \frac{v_{i,j}^2 (\Delta t)^2}{\bar{h}}$, with $\bar{h} = \sqrt{\frac{2}{\frac{1}{(\Delta x)^2} + \frac{1}{(\Delta z)^2}}}$

If $\Delta x = \Delta z = h$, the expression (11) reduces to

$$-1 \leq 1 + \bar{g}_{i,j} \left\{ \frac{(\cos(q\Delta y) - 1) + \frac{1}{36} [(2 + \cos(q\Delta y))(-\cos(2p\Delta x) + 16 \cos(p\Delta x) - 30)]}{1} \right\} \leq 1 \quad (12)$$

Therefore the stability condition should satisfy

$$\frac{v_{i,j} \Delta t}{h} \leq \sqrt{\frac{8}{13}}, \quad (13)$$

which is much weaker than the stability condition for a second order central FDM and fourth order central FDM (Larry Lines, etc, al., 1999). The comparison is shown as following Figure 2.

$$\frac{v_{i,j} \Delta t}{h} \leq \sqrt{\frac{8}{13}} \quad (\text{FE-FDM})$$

$$\frac{v_{i,j} \Delta t}{h} \leq \sqrt{\frac{6.5}{13}} \quad (\text{2nd order central FDM})$$

$$\frac{v_{i,j} \Delta t}{h} \leq \sqrt{\frac{4.875}{13}} \quad (\text{4th order central FDM})$$

Figure 2. The comparison between FE-FDM and traditional FDM

Hence, according to the above analysis of the stability condition, one finds that the algorithm based on the FE-FDM has a much less constraint stability condition than those based on conventional FDM under the same accuracy condition.

Absorbing boundary condition

The approach of the absorbing boundary condition (Clayton and Engquist, 1977) gives the fourth-order accuracy boundaries as following:

$$\text{Left side boundary: } \frac{\partial^2 u}{\partial x \partial t} - v \frac{\partial^2 u}{\partial t^2} + \frac{v}{2} \frac{\partial^2 u}{\partial z^2} = 0$$

$$\text{Right side boundary: } \frac{\partial^2 u}{\partial x \partial t} + v \frac{\partial^2 u}{\partial t^2} - \frac{v}{2} \frac{\partial^2 u}{\partial z^2} = 0$$

$$\text{Top boundary: } \frac{\partial^2 u}{\partial z \partial t} - v \frac{\partial^2 u}{\partial t^2} + \frac{v}{2} \frac{\partial^2 u}{\partial x^2} = 0$$

$$\text{Bottom boundary: } \frac{\partial^2 u}{\partial z \partial t} + v \frac{\partial^2 u}{\partial t^2} - \frac{v}{2} \frac{\partial^2 u}{\partial x^2} = 0.$$

For the migration, the value of the top boundary is the seismic section used to extrapolate the wavefield. So, the bottom boundary, left boundary and right boundary conditions are needed, which are same as the boundary conditions used with the wave modeling.

NUMERICAL EXAMPLES

In order to validity the algorithms of FE-FDM, some cases are chosen for modelling and migration. The numerical solution of modeling in a quarter-plane is compared with the corresponding analytical solution. One numerical case is designed to show the stability condition advantage of FE-FDM over FDM. For migration, a constant velocity model with two irregular interfaces is chosen to do modeling first and then migration.

Case I: Comparison between the numerical solution and analytical solution

The quarter-plane problem is a particular case of the infinite-wedge problem. As underlined by Wait (1959), the solution can be found by image theory. A source S inside the medium induces three virtual image sources, as shown in Figure 3. Two images S_x and S_z are symmetric with respect to the real source along the x-axis and z-axis edges. The third image S_c is symmetric of the real source with respect to the corner. For grid boundary condition on the two edges, one can write the solution at the point $M(x, z)$ as

$$G(x, z, t, x_s, z_s, t_s) * f(t_s) - G(x, z, t, x_s, -z_s, t_s) * f(t_s) - G(x, z, t, x_s, -z_s, t_s) * f(t_s) + G(x, z, t, -x_s, -z_s, t_s) * f(t_s).$$

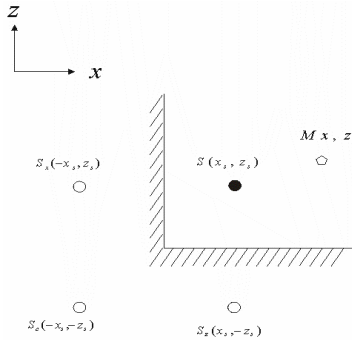


Figure 3. Quarter-plane geometry: Image theory interpretation

Table 1 gives the physical parameters of the quarter-plane problem. The usual rule of using at least ten points for the shortest wavelength of the source is respected for this scheme. The seismogram at a given point in Table 1 shows more quantitatively the accuracy of the numerical solution by comparison with the analytical solution in Figure 4. They are accurately matched except some difference in the amplitude.

Table 1: Quarter-plane parameters

Physical parameter	
Velocity	3000m/sec
Source and Observer position	$f_{main} = 50Hz$; source position: $250*250m^2$; observe position: $150*150m^2$.
Other parameters	$dx = 5m, dz = 5m, dt = 1.25E-3s$, grid of $300*300$ points

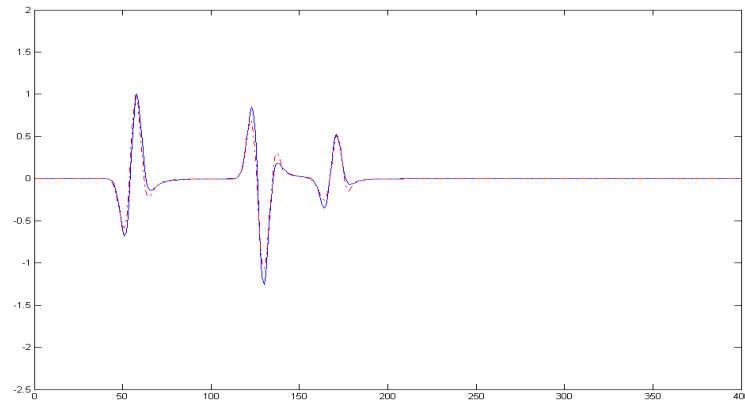


Figure 4. Seismogram at a given observer (Table 1). The solid blue line is the solution of analytical solution, and the dashed red line is the numerical solution of the FE-FDM

Case II: Comparison of stability condition between the FE-FDM and second order central FDM

To show the advantage of FE-FDM in a stable condition, we designed a homogenous model with the parameters in Table 2. According to the parameters and the previous analysis of the stability condition, we can know the computation of the 2nd order FDM scheme will diverge, while that of FE-FDM can still remain convergent, which is also proven from numerical simulation result of Figure 5 and Figure 6. Figure 5 is the result obtained from FE-FDM, and Figure 6 is from 2nd order FDM. From Figure 5, we can know the wave propagates outside from the source, while there is obvious numerical divergence by the traditional FD scheme from Figure 6.

Table 2: Parameters for modeling wave propagation

Physical parameter	
Velocity	1500m/sec
Source and Observer Position	$f_{main} = 50Hz$; source position: 150*150m ² ; observer time : 9ms.
Other parameters	$dx = 2m$, $dz = 2m$, $dt = 1.00E-3s$, grid of 300*300 points

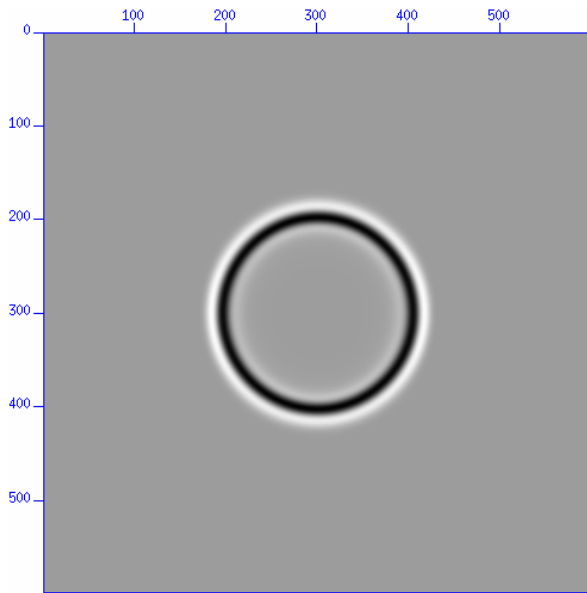


Figure 5. Modeling by FE-FDM.

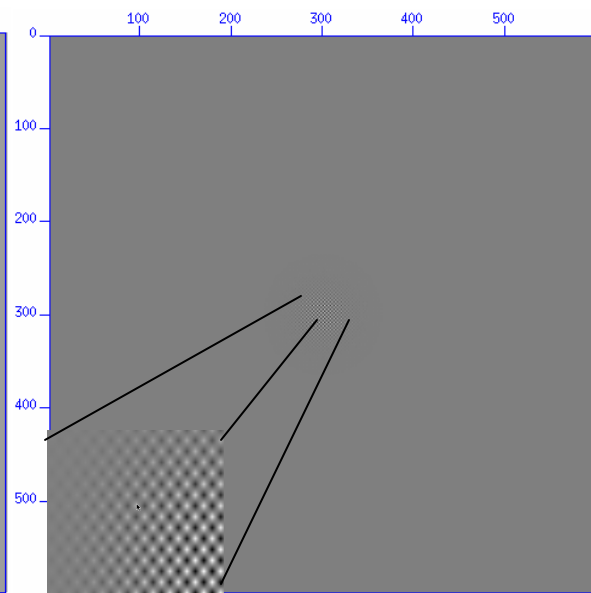


Figure 6. Same modeling by 2nd order central FDM

Case III: constant velocity migration with irregular interface

To test the image ability for the irregular interface, a constant velocity model with two irregular interfaces is designed, which is shown in Figure 7. The parameters of the model are shown in Table 3.

Table 2: the parameters of constant velocity model

Physical parameter	
Velocity	3000m/sec
Source and Observer position	Ricker wavelet with $f_{main} = 50\text{Hz}$; source: each point of the interfaces; observer: the line in the ground.
Other parameters	$dx = 3\text{m}$, $dz = 3\text{m}$, $dt = 1.0\text{E-}3\text{s}$, grid of 500*300 points

Using the FE-FDM, the exploding reflection model (ERM) and the parameters shown above, one can get the post-stack seismic section, which is shown in Figure 8. Figure 9 is the migration result. Compared with the model in Figure 7, there is a good corresponding relationship between the migration result and the model. The FE-FDM migration images the irregular interfaces and accurately locates the diffraction in the right place. In addition, there is some weak diffraction in the migration section because of the truncation, but it doesn't affect the image result. Therefore, the FE-FDM can work well under the cases with the constant velocity.

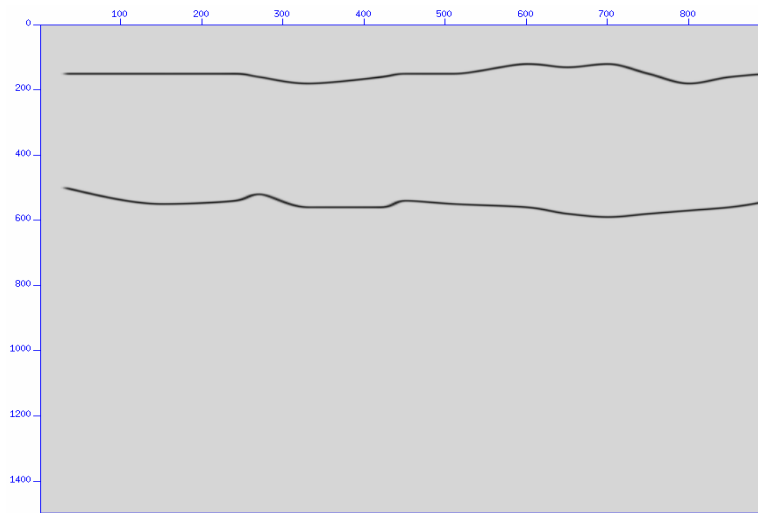


Figure 7. The complex velocity model with irregular interfaces

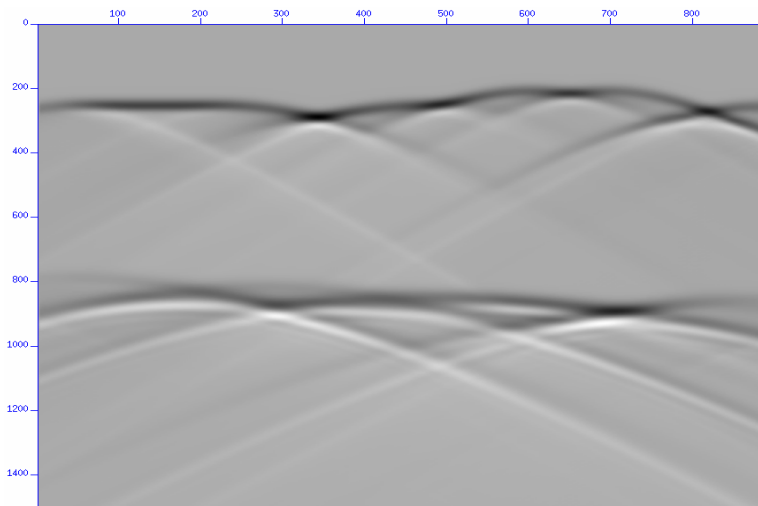


Figure 8. The seismogram generated by the FE-FDM

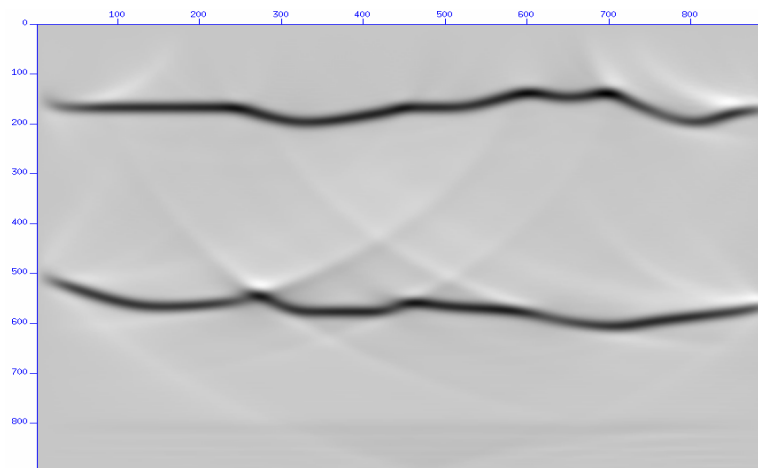


Figure 9. The migration result from using the FE-FDM

CONCLUSIONS

A numerical method named finite element–finite difference method (FE-FDM) for the solution of full 2-D wave equation is presented in this paper. Numerical examples of 2-D acoustic wave equation modeling and reverse-time depth migration were shown illustriously that the result is accurate and effective for the simulation of a complex wavefield and migration of the irregular interfaces. This method combines FEM and FDM based upon the semi-discretization of the spatial domain. The main strengths of FEM (adaptation to arbitrary domain) and FDM (computation efficiency) are inherited. FE-FDM has a more relaxed stability condition than the FDM with the same accuracy. The application of a good absorbing boundary condition contributes to better imaging ability in the modelling and migration. It is therefore a useful and promising numerical method.

ACKNOWLEDGEMENTS

We should thank Dong Yuan of Tsinghua University for he firstly developed this method and provide us with information, which motivated our research in this area. We also sincerely express gratitude to Larry Lines, and Edward S. Krebs and Chuck Ursenbach for many helpful discussions. At last, we should express thanks for the CREWES project.

REFERENCES

- Clayton R. and Engquist, B., 1977, Absorbing boundary condition for acoustic and elastic wave equations: Bulletin of the Seismological Society of America, Volume 67:6, 1529-1540
- Dong Y., 2000, Multi-wave NMO velocity fracture detection and finite element – finite difference reverse time migration, Ph.D thesis: Tsinghua University.
- Durrant, D. R., Numerical methods for wave equations in geophysical fluid dynamics, Springer-Verlag New York, Inc. 1999.
- Lines, R., Slawinski R. and Bording P., A recipe for stability of finite-difference wave-equation computations: Geophysics, 64, 967-969
- Lu, J. and Guan, Z., 1987 Numerical method of partial differential equations (In Chinese), Beijing: Tsinghua University Press.
- Wait, J. R., 1959, Eletro-magnetic radiation from cylindrical structure: Pergamon Press Inc.
- Wu, W., Lines, L. R., and Lu, H., 1996, Analysis of higher-order finite difference schemes in 3-D reverse-time migration: Geophysics, 61, 845–856.